

Impact of lockdown due to COVID-19 outbreak on O₃ and its precursor gases, PM and BC over northeast India

Binita Pathak^{1,2,*}, Pradip Kumar Bhuyan², Arshini Saikia², Kalyan Bhuyan^{1,2}, P. Ajay², Sankar Jyoti Nath² and Shyam Lochan Bora¹

¹Department of Physics, Dibrugarh University, Dibrugarh 786 004, India

²Centre for Atmospheric Studies, Dibrugarh University, Dibrugarh 786 004, India

Copernicus Atmosphere Monitoring Service (CAMS) data are used to evaluate the impact of the lockdown (24 March–3 May 2020) on the concentrations of surface O₃, NO_x, CO, SO₂, PM and BC compared to those measured during the same period in 2015–2019 over northeast India and adjoining areas. Measurements made at Dibrugarh complements the CAMS observations. The NO_x, NO₂, CO, SO₂, BC and PM concentrations dipped appreciably over northeast India and nearby countries. Similar decrement is observed in Dibrugarh in 2020 over their reference levels. Reduction of precursor gases triggered an increase in O₃ concentration across northeast India and adjoining South Asia and at Dibrugarh. The air quality over the region improved from moderate to satisfactory levels due to the lockdown.

Keywords: Aerosols, air quality, COVID-19, lockdown, northeast India, particulate matter, trace gases.

Introduction

THE pneumonia virus (later on christened COVID-19), that originated in the Wuhan province of China in December 2019 was declared by the WHO on 30 January 2020 as a public health emergency of international concern. It became a full scale epidemic in China by February–March 2020 and simultaneously in many parts of the world including Western Europe and North America. The virus spread thick and fast across all continents and affected millions of people. As of 8 June 2020, around 7 million people have been infected in 216 countries and 4 hundred thousand have lost their lives due to the pandemic. In India, a few cases were detected on 30 January and the number continued to increase as days passed by and became a matter of great concern. The COVID-19 virus spreads from human to human in close proximity, as aerosol droplets of different sizes. Therefore, to prevent the spread of the pandemic many countries banned all outdoor activities including travel. People were confined

to their homes for specified periods after assessment of the threat perceptions at national levels. In India lockdown was first imposed from 24 March to 14 April as phase I and then extended from 15 April to 3 May as phase II. All restrictions imposed in phase I remained in place for phase II thus putting the entire country to stand still for 40 days. Though the confinement has disadvantaged all sections of the society and people of all age groups, it also provided an opportunity to environmentalists and atmospheric scientists to assess the positive impact of cessation of a significant amount of anthropogenic activities, viz. vehicular movement, closure of industries, biomass burning on the environment.

The impact of the lockdown primarily on air quality has been examined by a number of researchers so far. For example, the response of air quality due to decrease in Chinese economic activities during January–February 2020 was examined¹ and a strong reduction in the emission of primary air pollutants was found. Surface measurements at about 800 stations showed that PM_{2.5} and NO₂ decreased by ~35% and ~60% respectively, from 1 January to 29 February 2020. Simultaneously, the mean O₃ concentration increased by a factor of 1.5–2. The impact of COVID-19 on air quality was assessed² in Central China and observed that the mean concentration of PM_{2.5}, PM₁₀, SO₂, CO and NO₂ in three cities: Wuhan, Jingmen and Enshi were lowered by 30.1%, 40.5%, 33.4%, 27.9%, 61.4% respectively, from the level in 2017–2019. Simultaneously, O₃ increased by 11–14% between January and March. On the other hand, Bauwens *et al.*³ used column NO₂ measured by the TROPOMI and OMI to study the effect of the coronavirus pandemic on NO₂ level over selected cities. Satellite NO₂ data shows about 40% decrease over Chinese cities while Western Europe and US displayed 22–38% NO₂ reduction in 2020 relative to the same period in 2019. However, over Iran, a region strongly affected by the outbreak no appreciable reduction in emission was observed. Positive impact of lockdown on air pollution over India has also been reported^{4,5}.

Earlier studies^{6–8} over Dibrugarh (27.4°N, 94.9°E), situated in the upper Brahmaputra basin of the northeast India have established that the aerosol and gas load peak

*For correspondence. (e-mail: pathak.binita8@gmail.com)

during February–March and decay thereafter in the rest of the pre-monsoon and monsoon seasons. Though there is certain annual variation in the amount of total pollutant concentration, the decreasing trend from winter to monsoon is consistent in all years. Therefore, we assess here the impact of the lockdown on the near surface gaseous and particulate matter pollutants: O₃, NO₂, NO_x, CO, SO₂, PM₁₀, PM_{2.5}, PM₁ and BC over northeast India by comparing the CAMS near real time data obtained from 24 March to 3 May 2020 with those obtained in the same period of preceding years (24 March–3 May of 2015–2019), which is considered as the reference period. Thereby, the influence of the natural seasonal decreasing trend on the pollutant level in the lockdown period is circumvented. Surface measurements of trace gases and aerosols (PM and BC) made at Dibrugarh are further used to complement the results inferred from CAMS NRT analysis.

Study domain and data

Study domain

The study region (Figure 1 *a* and *b*) within the geographical boundaries of 20°N–30°N and 86°E–100°E comprises northeast India, Bhutan, parts of Myanmar, Bangladesh and parts of West Bengal. The primary focus is in northeast India which is in the transition region between South and Southeast Asia. It is also the easternmost region of India consisting of eight states: Arunachal Pradesh, Assam, Manipur, Meghalaya, Mizoram, Nagaland, Tripura and Sikkim covering an area of 262,179 sq. km, where nearly 65% of the total geographical area is covered by forest. The altitude of the region varies from 50 m above mean sea level (amsl) in the lower Brahmaputra region to higher heights of 7000 m amsl in the eastern Himalaya. Rocky surface, alpine vegetation and snow-capped high peaks dominate the physical landscape of this region where 72% of the area is under hilly ecosystem. Biomass burning, especially as a part of shifting cultivation (Jhuming), involving burning of stretches of forests and growing a number of crops is widely practiced in this region down south and it, along with brick kilns (coal-fired), open coal mining and oil and gas fields make this region a strong source of anthropogenic emissions. Biomass burning releases a huge amount of BC and trace gases, which peaks in the month of March–April^{7,9}. Open coal mining, brick kilns, oil and gas fields contribute to carbonaceous aerosols and trace gases. Large vegetation in the North-Eastern region is a good source of volatile organic compounds (VOCs) along with biological aerosols¹⁰. The region is also rich in soil organic carbon. Earlier studies^{11–15} have shown how transportation from IGP, mainland and western India and western Asia intensifies the aerosol loading in the region, particularly during the pre-monsoon (MAM) season. The eastern IGP, encompassing West Bengal and parts of Bangladesh are highly popu-

lated and anthropogenic activities dominate emission of pollutant gases and aerosols. Bhutan is topographically and anthropogenically akin to the NE states of Sikkim and Arunachal Pradesh. North-East Myanmar is sparsely populated and biogenic activities predominate. In this study, parts of eastern IGP (West Bengal and Bangladesh) in the west and Myanmar in the east have been included as they exert significant influence upon the pollutant load of north-east India¹³.

Data source: Copernicus atmosphere monitoring service

The Copernicus atmosphere monitoring service (CAMS) global real time production system provides daily near-real-time (NRT) analyses and forecasts of global atmospheric composition (aerosols, reactive and greenhouse gases, stratospheric ozone and related species, and UV radiation). Here satellite observations are combined using the four-dimensional variational (4D-VAR) data assimilation technique with chemistry-aerosol modelling to obtain the mass mixing ratios of atmospheric trace gases and aerosols¹⁶. The analyses are available at 6-hourly (00, 06, 12, 18 UT) intervals at different spatial resolutions. CAMS system is based on the Integrated Forecasting System (IFS) of the European Centre for Medium-Range Weather Forecasts (ECMWF), which was extended to provide daily forecasts, and reanalyses of atmospheric composition, by combining ground-based and satellite observations of atmospheric composition with state-of-the-art atmospheric modelling. CAMS data are evaluated against Global Atmosphere Watch (GAW) Surface Observations and the NOAA Earth System Research Laboratory (ESRL) for ground-based O₃ concentrations, which shows biases of ~24% over the USA and tropical stations. In case of NO₂, the SCIAMACHY/Envisat and GOME-2/MetOp-A NO₂ data are well reproduced by the NRT model runs, indicating that emission patterns and NO_x photochemistry are represented well. All model runs underestimate CO surface concentrations with mean biases with respect to GAW up to –15%. The details of the data are available at <http://www.copernicus.atmosphere.eu/validation>.

In the present study, we have used CAMS air pollutants (O₃, NO_x, NO₂, CO, SO₂ and BC) datasets at a horizontal resolution of 0.125° × 0.125° during 24 March–3 May of the years 2015–2020 at 6-hourly intervals, 0 time steps (<https://apps.ecmwf.int/datasets/data/cams-nrealtime/levtype=pl/>). The particulate matter (PM₁, PM_{2.5} and PM₁₀) data are available at 12 hour intervals, 0 time steps with a horizontal resolution of 0.125° × 0.125° since 2018 (<https://apps.ecmwf.int/datasets/data/cams-nrealtime/levtype=sfc/>). Therefore, for these species 2018–2020 data are used. Satellite/Model reanalysis data are being increasingly used by the scientific community for better spatial and temporal coverage^{17,18} or used for

forecasting¹⁹, despite certain uncertainties involved due to assumptions and algorithms used in the process. Satellite or model data can be validated by ground measurements. For example, Girach *et al.*¹⁸ used *in-situ* CO measurements in the Indian Ocean during January–February 2018 and found good agreement with Measure-

ments of Pollution in the Troposphere (MOPITT) version 8 retrieved data and CAMS model results. Saikia *et al.*¹⁶ evaluated the performance of the Weather Research and Forecasting model coupled with chemistry (WRF-Chem), the WRF coupled with Sulfur Transport dEposition Model (WRF-STEM), and CAMS model for the meteorological

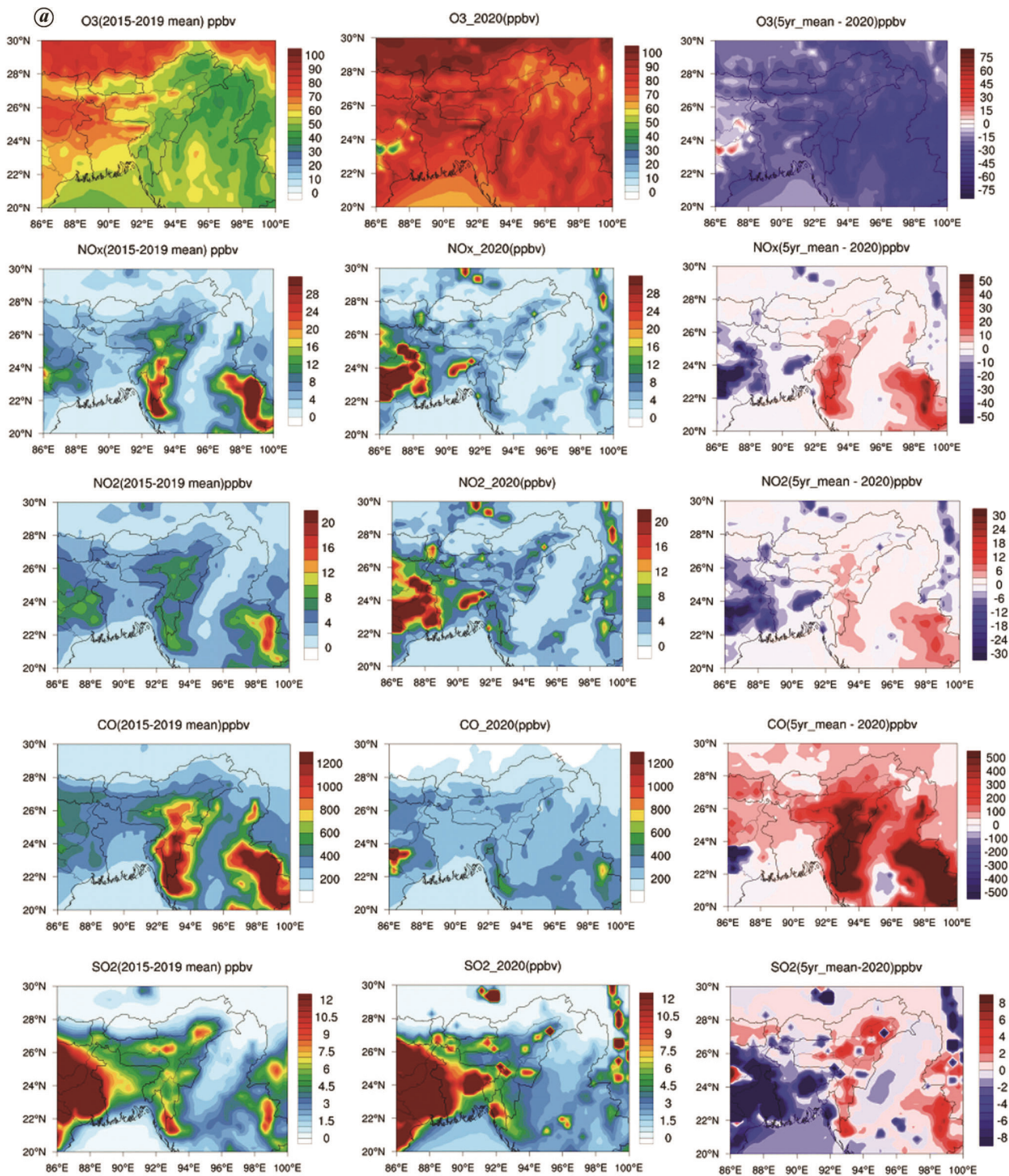


Figure 1. a, Spatial distribution of gaseous pollutants over northeast and adjoining areas within the selected domain.

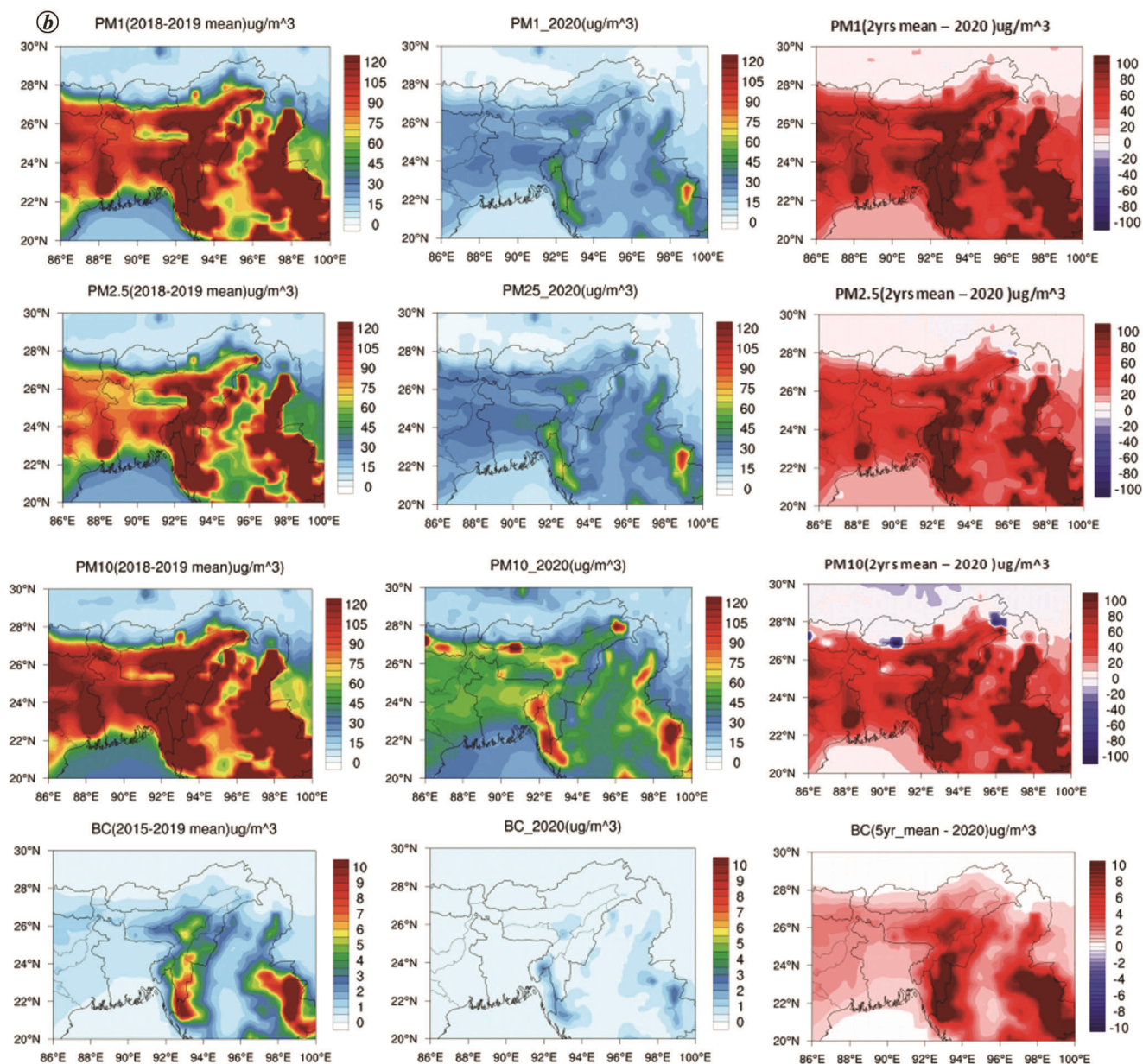


Figure 1. b, Spatial distribution of particulate matter and black carbon over northeast India and adjoining areas within the selected domain.

variables and air pollutants BC, CO, SO₂, O₃, and NO_x made observations at Dibrugarh and found good compatibility.

Surface measurements

O₃, NO_x and CO concentrations are collected at a temporal resolution of 5 min in Dibrugarh using O₃ (T400) and NO_x (T200), CO (T300) Teledyne API analysers. The O₃ and CO analysers work on the principle of absorption of ultraviolet light at 254 nm and infrared absorption at 4.7 nm respectively. The NO_x analyser is based on the chemiluminescence at 630 nm produced by the oxidation of NO by O₃ molecules. The BC data is also collected at

5 min interval over Dibrugarh using an Aethalometer, that measures attenuation of a light beam at seven wavelengths (370, 470, 520, 590, 660, 880 and 950 nm) at a flow rate of 3 l/min. Observations at the 880 nm wavelength are considered standard for BC measurement as it is the principal absorber of light at this wavelength, whereas other aerosol components have negligible absorption. Further details of all the instruments can be found elsewhere^{7,8,20} and references therein. The PM₁ concentration is derived from the number-size distribution of aerosols in the size range 1 nm–1 μm at 192 bins, obtained from a Nano-Scanning Mobility Particle Sizer (nano-SMPS, Model No 3938L72 TSI Inc., USA) at 5 min time resolution. The density of aerosols considered

here is 2 g/cm^3 which is typical for continental aerosol²⁰. The SMPS measures the aerosol number size using the principle of ‘differential mobility analysis’ of aerosol particles. A long and reliable database of these species, with some gaps for operational reasons, exists which are being used as a reference for measurement done during the lockdown period. The reference period considered is 2012–2019 for trace gases, 2015–2019 for BC and 2019 for PM₁.

Results and discussion

Spatial distribution of pollutants

The concentration of both gaseous pollutants and particulate matter is moderately high in north-east India^{11–15} despite the fact that the region is comparatively less populated and industrial and anthropogenic activities are low compared to rest of India, particularly the industrialized west and highly populated Indo-Gangetic plains (IGP).

Figure 1 *a* illustrates the spatial distribution of O₃, NO_x, NO₂, CO and SO₂ over northeast India and adjoining areas for the period 2015–2019, 2020 and their biases. Spatially, O₃ is high in the areas west of 92°E and low towards east during 2015–2019. In 2020, O₃ in the east increased more as compared to that in the west. The difference in O₃ concentration was higher towards east of 92°E, which indicates that during the lockdown period more O₃ was produced in the east, the region with more vegetation and lowest population density as compared to the west that comprises parts of the highly polluted IGP and Bangladesh. The distribution of nitrogen oxides illustrates the uneven concentration of the species both in 2020 and during 2015–2019. In 2015–2019, NO₂ is high (~10 ppb) in the eastern IGP and southern stretches of northeast India and highest (~18 ppb) in parts of Myanmar. NO₂ concentration in other parts of the region remained low (<6 ppb). The spatial variation of NO_x is similar to that of the dominant component NO₂. During 2015–2019, NO_x was high in southern Assam, Mizoram and northeast Myanmar compared to the level in other areas.

The concentration of CO is very high in southern stretches of northeast India and northeast Myanmar during 2015–2019. In 2020, no CO hotspot is observed over the entire region except in a small area in eastern IGP. The absence of NO_x, NO₂ and CO hotspots during 2020 demonstrates the impact of lockdown with cessation of anthropogenic burning over those areas. SO₂, on the other hand, does not vary much during the lockdown period from the five-year average, the bias being only up to –8 ppb. During both the periods, SO₂ is higher in the eastern IGP and parts of Bangladesh. This may be attributed to the SO₂ emissions from the coal-based thermal power plants (operational during the lockdown period) clustered around the eastern IGP²¹. The spatial spread of

SO₂ in the lockdown period along with hotspots of NO_x, NO₂ and CO in the eastern IGP signifies intensification of emission of all the species. This may be attributed to emission from unattended industries due to lockdown. Further, the scattered small hotspots of SO₂ during both 2015–2019 and 2020 may be due to the scattered oil and gas fields in northeast India.

The impact of lockdown is also prominent from the spatial distribution of aerosol species: PM₁₀, PM_{2.5}, PM₁ and BC (Figure 1 *b*), with drastic reduction in 2020 from their level in 2018–2019. The spatial distribution of PM₁ and PM_{2.5} is similar across the region both during 2018–2019 and 2020, whereas PM₁₀ exhibits some small hotspots across the region even in 2020. As expected, the spatial distribution of BC follows the same pattern as NO_x, NO₂ and CO during both the periods. The hotspots of these species over southern Assam, Mizoram and Myanmar are also visible for all PM species. Thus it is evident that, anthropogenic biomass burning, i.e. Jhuming was absent during lockdown in these areas, which otherwise peaks in March–April of each year. During the lockdown outdoor activity was restricted and it is reasonable to believe that in the absence of biomass burning to the extent it is normally practised, BC emission was limited to a very low level.

In order to quantify the impact of lockdown, i.e. cessation of anthropogenic activities on the level of pollutant gases and aerosols, the concentrations are spatially averaged over the entire domain for both reference (2015–2019) and the lockdown (2020) periods and are presented in Figure 2. It is seen that mean O₃ mixing ratio increased

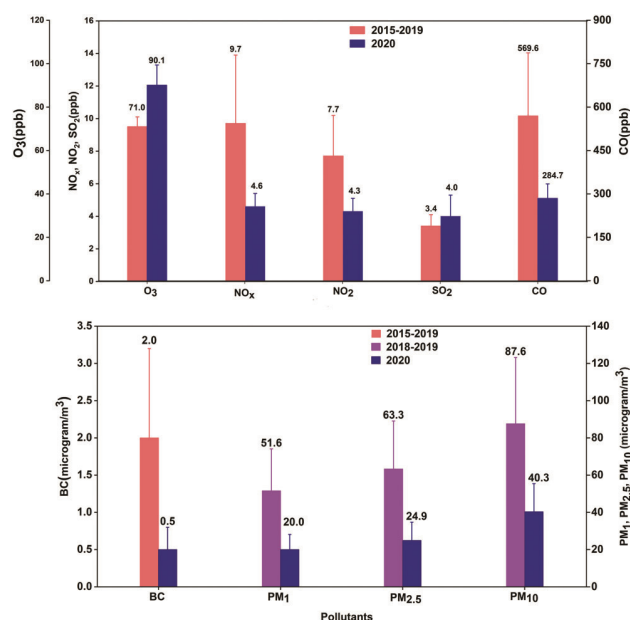


Figure 2. Mean concentration for trace gases and aerosols averaged spatially for the whole domain during 2015–2019 and 2020. The vertical lines indicate year to year variation during 2015–2019 for O₃, NO_x, NO₂, CO, SO₂ and BC and during 2018–2019 for PMs and day to day variation in 2020.

by 38% from 70.9 ppb in reference period to 90.08 ppb in lockdown period (Figure 2 a). The minimum and maximum concentrations of O₃ in 2015–2019 are 63.0 ppb and 78.8 ppb whereas in 2020 it varied from 74.8 ppb to 105.7 ppb respectively. On the other hand, the concentration of the precursor gases NO₂, NO_x (NO₂ + NO) and CO decreased substantially during the lockdown. The NO₂ concentration of 7.65 ppb in 2015–2019 reduced to 4.3 ppb in 2020, i.e. a decrement of ~43%. The minimum and maximum NO₂ concentrations ranged between 0.47 ppb and 61.5 ppb in 2015–2019 and between 0.41 ppb and 11.45 ppb in 2020. Similarly, mean NO_x concentration of 9.7 ppb in 2015–2019 reduced to 4.62 ppb in 2020. The decrease due to the lockdown in NO_x is by ~52% over the reference level. The concentration of NO_x ranged between 0.55 ppb and 75.7 ppb during 2015–2019 and between 0.51 ppb and 12.8 ppb in 2020. The reduction in NO is rather drastic (~84%), i.e. its abundance becomes nearly insignificant, thus having major implications on O₃ production/loss. CO too exhibits a decline in concentration from 570 ppb to 285 ppb, a decrease of 50% over the preceding 5-year period. CO concentration varied largely from a minimum of 176.2 ppb to a maximum of 4112.16 ppb in 2015–2019 and between 165.7 ppb and 560.4 ppb in 2020. However SO₂ increased marginally (~17%) during the lockdown from 3.42 ppb (2015–2019) to 4.02 ppb (2020).

The PM concentration in all size ranges shrunk during lockdown as shown in Figure 2 b. PM₁ mean concentration of 51.6 µg m⁻³ in 2018–2019 was reduced by 61% to 19.9 µg m⁻³ in 2020. The minimum–maximum variation in PM₁ during 2018–2019 was 12.2–193.7 and 7.99–44.4 µg m⁻³ in 2020. PM_{2.5} concentration of 63.3 µg m⁻³ decreased by ~61% to 24.9 µg m⁻³. PM_{2.5} ranged from the minimum value of 18.6 µg m⁻³ to 223.6 µg m⁻³ in 2018–19 and from 10.2 µg m⁻³ to 54.2 µg m⁻³ in 2020. PM₁₀ also reduced by ~54% from 87.6 µg m⁻³ (2018–19) to 40.3 µg m⁻³ (2020). PM₁₀ concentration varied between 25.8 µg m⁻³ and 309.0 µg m⁻³ in 2018–19 and between 16.9 µg m⁻³ and 84.9 µg m⁻³ in 2020. A major source of PMs over the region is anthropogenic dust including road dust associated with the transport sector. Thus, the drastic reduction in PM levels during the lockdown period could be partially attributed to the absence of vehicles and trains. BC during the same period decreased by 76% from the average value of 1.87 µg m⁻³ in 2015–2019 to 0.44 µg m⁻³ in 2020. It is, therefore, seen that among all the aerosol species the impact of the lockdown on BC was the most drastic, due to absence of biomass burning as discussed earlier.

Trends in air pollutants during the lockdown period

In addition to the inherent natural trend of the pollutants, the trends induced, if any, by the lockdown is studied.

The magnitude of trend in the time series has been determined by the familiar nonparametric method. Sen's estimator and statistical significance of the trend has been evaluated by Mann–Kendall (MK) test²². It has been found (Table 1) that the pollutants CO, NO_x, PM₁, PM_{2.5} and PM₁₀ show statistically significant decreasing trends during phase I and phase II of the lockdown. BC even though exhibits a statistically significant decreasing trend in the phase I of lockdown, during the phase II it shows an insignificant increasing trend. O₃ exhibits decreasing trends during both the phases, but is statistically insignificant in phase I and significant in phase II. SO₂ shows statistically non-significant decreasing trends in both the phases of lockdown. Moreover, during the whole lockdown period (phase I + phase II), all the pollutants show statistically significant decreasing trends.

A comparison of the trends in the average values of the pollutants during the reference period (2015–2019 for BC, CO, NO_x, SO₂, O₃ and 2018–2019 for PM₁, PM_{2.5}, PM₁₀) reveals insignificant decreasing trends for BC, CO, NO_x, O₃ during 24 March–14 April and from 15 April to 3 May. On the other hand, SO₂ exhibits a decreasing trend during the period from 24 March to 14 April and an increasing trend during 15 April–3 May, however, the trends are statistically non-significant. The pollutants PM₁, PM_{2.5}, PM₁₀ show statistically significant decreasing trends during both the periods. However, for the entire reference period, all the species exhibit statistically significant decreasing trends except O₃, whose decreasing trend is statistically insignificant. The impact of the lockdown on the pollutant level as it appears is not instantaneous rather gradual. As the pollutants are emitted to the atmosphere from multiple sources at different emission rates and multiple reactions occur between these species, their levels are not expected to be impacted very fast, which is reflected in the observed trend during the period of the lockdown. Further, factors like effect of meteorology have not been considered, e.g. the entire northeast India was under severe thunderstorm activity from 14 April onwards for almost two weeks that impacted solar radiation and hence production of O₃. The concentration of both gases and PM peaks in winter and gradually reduces through pre-monsoon.

Variation of gases and aerosols over Dibrugarh

The variations of the measured trace gases (upper panel) and aerosols (lower panel) over Dibrugarh are similar to that observed for entire northeast India (Figure 3). O₃ increased from 27.7 ppb in 2012–2019 to 40.1 ppb in 2020. Simultaneously NO₂ decreased from 12.6 ppb to 7.9 ppb and NO_x concentration came down from 16.1 ppb to 9.5 ppb to due to lockdown. CO decreased from 785.4 ppb to 275.2 ppb. The deviation in 2020 from the previous years is 45%, -41%, -37% and -65%

Table 1. Trends in pollutants (Sen's slope values). The italics indicate statistically significant values

Pollutant	Trends in pollutants during lockdown period			Trends in pollutants during the reference period (average of previous years)		
	Phase I (24 March–14 April)	Phase II (15 April–3 May)	During whole lockdown	24 March– 14 April	15 April– 3 May	During whole period
BC	-0.022	0.020	-0.012	-0.098 ^a	-0.035 ^a	-0.056 ^a
CO	-2.649	-4.146	-3.064	-20.050 ^a	-0.320 ^a	-8.948 ^a
NO _x	-0.061	-0.071	-0.049	-0.363 ^a	-0.162 ^a	-0.228 ^a
O ₃	-0.064	-0.520	-0.682	-0.243 ^a	-0.049 ^a	-0.091 ^a
SO ₂	-0.059	-0.040	-0.100	-0.040 ^a	0.012 ^a	-0.031 ^a
PM ₁	-0.429	-0.499	-0.578	-3.163 ^b	-1.689 ^b	-1.616 ^b
PM _{2.5}	-0.465	-0.644	-0.704	-3.640 ^b	-1.924 ^b	-1.833 ^b
PM ₁₀	-0.520	-1.049	-1.088	-5.154 ^b	-2.691 ^b	-2.53 ^b

^aPeriod 2015–2019; ^bPeriod 2018–2019.

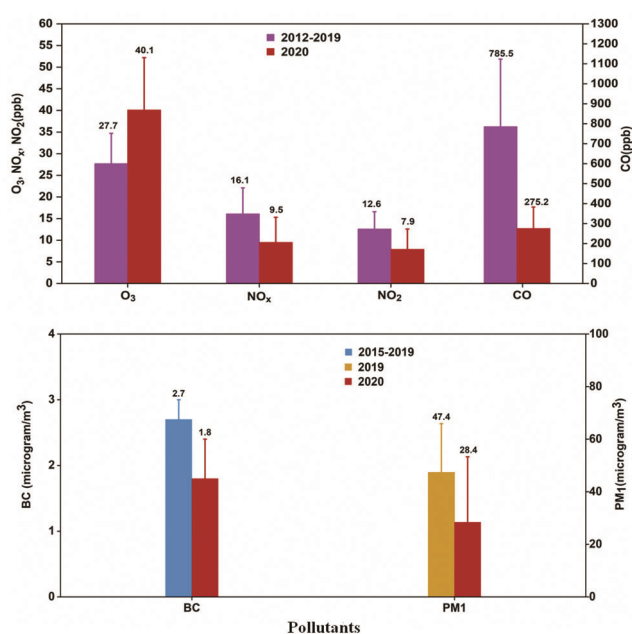


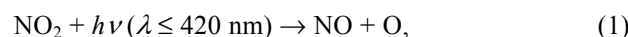
Figure 3. Mean concentration for trace gases and aerosols measured over Dibrugarh during 2015–2019 and 2020. The vertical bars indicate year to year variation during 2015–2019, day to day variation in 2020 for O₃, NO_x, NO₂, CO, SO₂ and BC and day to day variation for PM₁.

respectively for O₃, NO_x and CO. The corresponding values for the entire domain are +38%, -52% -43% and -50% respectively. Similarly, the decrement is appreciable for PM₁ (-40%) and BC (-35.6%) over Dibrugarh. The increment and decrement of the trace gases and aerosols over Dibrugarh due to lockdown are true reflection of their behaviour with reasonable differences in magnitude brought about by the spatial variation in concentration of each species.

Why has O₃ increased?

As has been observed, the average concentration of surface O₃ during the lockdown is appreciably higher than

that observed in the same period in the preceding years. This increase in O₃ is due to the simultaneous decrease in NO_x as a result of the absence of outdoor anthropogenic activities mainly vehicular movement and industries other than power plants. O₃ and NO_x are inextricably linked due to the chemical coupling between the two under sufficiently intense solar radiation. NO₂ is first dissociated into NO and O via the following reaction leading to production of O₃.



NO react with O₃ to produce NO₂ and reduce O₃



Thus, NO again removes O₃ from the atmosphere (eq. (3)). From chemistry climate model analysis²³ and from surface measurements⁸, it was found that at low NO_x concentration O₃ production is limited by the availability of NO_x molecule. When concentration is high, other compounds limit the O₃ production, i.e. HO_x radicals through reactions with NO_x. Thus, O₃ and NO_x are nonlinearly related. Bhuyan *et al.*⁸ observed that the correlation between average NO_x and O₃ over a certain local time period is the result of the combined effect of chemical reaction, transport patterns, atmospheric dispersion, etc. During the daytime, NO_x concentration is low as it undergoes photochemical reaction to produce O₃, whereas at night in the absence of sunlight, titration reaction between O₃ and NO leads to destruction of O₃. Over Dibrugarh O₃ and the NO_x are nonlinearly related when the production/loss mechanisms are considered for entire 24 hours (Figure 4). The nonlinearity between the two is produced by a combination of linear negative correlation for NO_x < 5 ppb and as O₃ is reduced to low level at high NO_x concentration no correlation exists. So, this is suggestive of the O₃ production process governed by NO_x

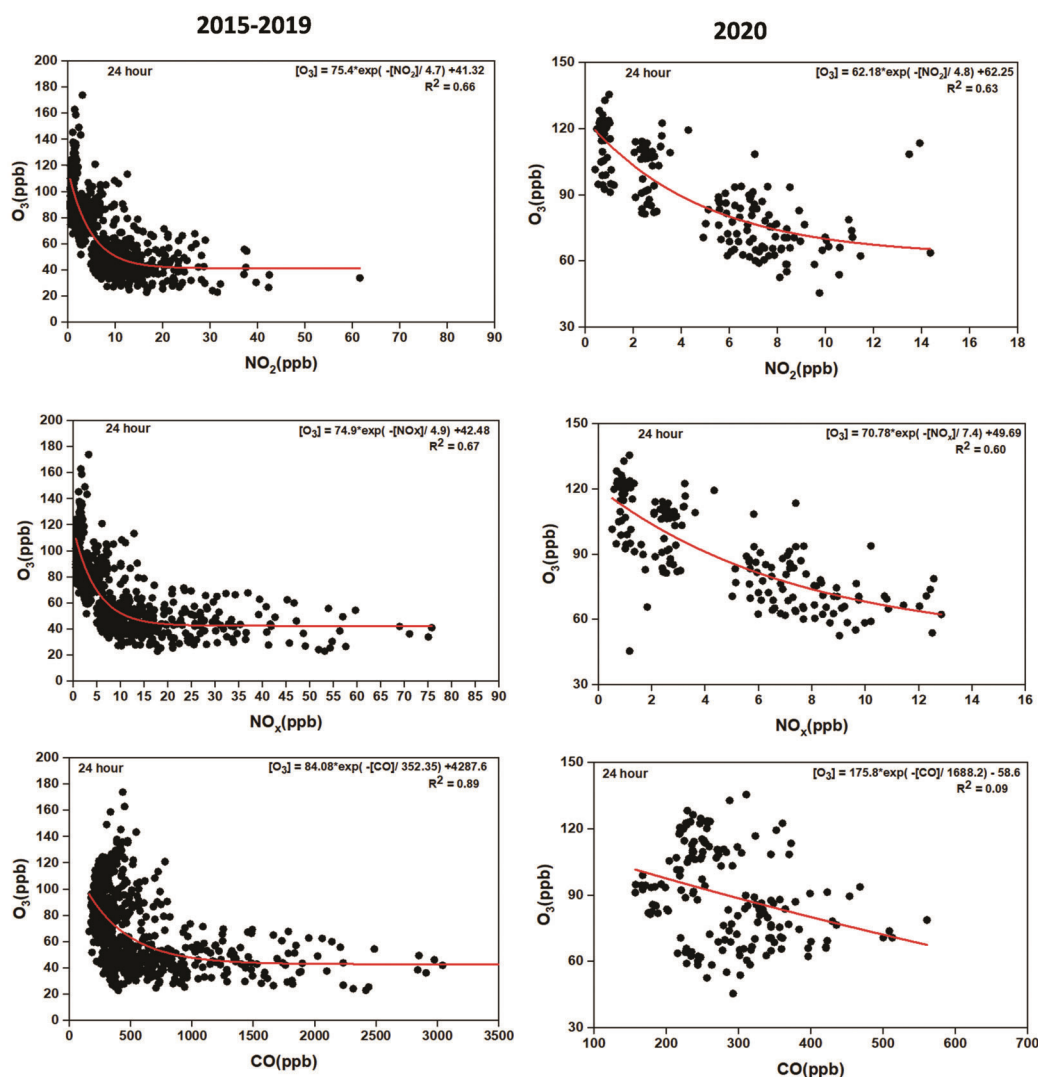


Figure 4. Scatter plot of O₃ with NO₂, NO_x and CO for 2015–2019 (left panels) and 2020 (right panels). The solid lines are the nonlinear regressions through the data points.

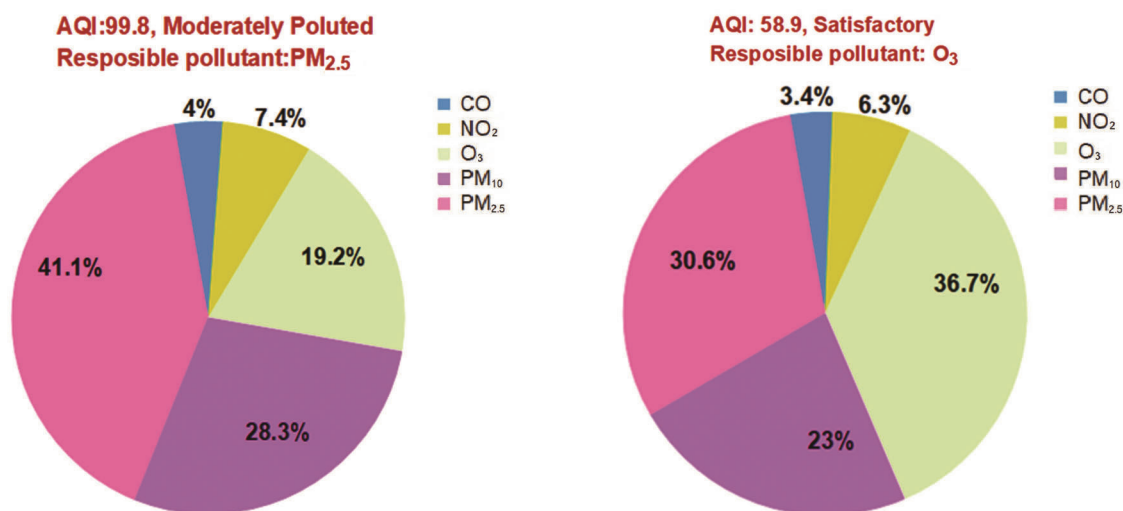
saturated and VOC sensitive regime^{8,24}. In an NO_x saturated regime, its concentration being high, the rate of OH + NO₂ termination reaction increases as NO_x increases removing both HO_x and NO_x from the system limiting the OH and OH₂ cycling, thus decreasing the rate of O₃ production. Further, there may be a simultaneous decrease in O₃ and NO_x due to the reaction of NO with O₃ to form NO₂ which further reacts with NO₃ radical to produce N₂O₅. It has also been observed that at Dibrugarh NO₂ and NO are strongly positively related, therefore, a significant correlation of NO_x with both NO₂ and NO exists. This explains the observed similar spatial variation of NO_x and NO₂ in the present study. During April both in 2015–2019 and 2020, O₃ remains nearly nonvariant with increase in NO_x.

The other precursor CO influences the production and loss of O₃ depending on NO₂ and NO_x concentrations²⁵.

The sources of CO are combustion of fossil fuel, oxidation of methane and anthropogenic and biogenic hydrocarbon and biomass burning²⁶. It acts as an intermediary in the oxidation cycle of hydrocarbons and methane and alters the oxidizing capacity of the atmosphere as it acts as a main sink for OH in the troposphere. High concentration of CO poses major threat to human health and can cause hypoxia leading to dizziness and even death. Further, the role of CO and O₃ was examined⁸ and a non-linear negative relationship was found between the two. During the day, CO are removed from the atmosphere through oxidation reactions to produce O₃. Thus O₃ and CO are negatively correlated for CO mixing ratio up to 1 ppm. The drastic reduction in CO in 2020 contributed to the observed increase in O₃. Figure 4 shows that O₃ is negatively correlated with the precursor gases which explains the observed increase in O₃ concentration during

Table 2. Categorization of air quality based on AQI values as defined by the CPCB²⁶

Good	Satisfactory	Moderately polluted	Poor	Very poor	Severe
0–50	51–100	101–200	201–300	301–400	401–500

**Figure 5.** Relative contribution of pollutant gases and particulate matter to the air quality index as defined by the Central Pollution Control Board of India for the period (a) 2015–2019 and (b) 2020.

the lockdown as precursor concentrations reduced substantially.

Impact of lockdown on regional air quality

In order to examine impact of the lockdown on possible improvement in air quality, over the region, the Air Quality Index (AQI), as defined by the Central Pollution Control Board of India has been estimated for 24 March–3 May of 2015–2019 and 2020 separately and shown in Figure 5. AQI for any species i is defined as

$$I_i = \left[\left\{ \frac{(I_{HI} - I_{LO})}{(B_{HI} - B_{LO})} \right\} * (I_p - B_{LO}) \right] + I_{LO}, \quad (4)$$

where B_{HI} is the breakpoint concentration greater or equal to given concentration; B_{LO} the breakpoint concentration smaller or equal to given concentration; I_{HI} the AQI value corresponding to B_{HI} ; I_{LO} the AQI value corresponding to B_{LO} ; I_p is the pollutant concentration.

AQI is then calculated as

$$AQI = \text{Max} (I_1, I_2, I_3, \dots, I_n). \quad (5)$$

Based on aggregate value of AQI, air quality is considered as²⁷ good to severe (Table 2).

The air quality for reference period in 2015–2019 over northeast India and adjoining areas was moderately polluted (Figure 5 a) in which the dominant pollutant PM_{2.5}

had 43.8% contribution. Among the gases, O₃ has highest contribution of 16.5%. On the other hand, the air quality across the region improved to satisfactory level in 2020 (Figure 5 b) in which O₃ became the dominant pollutant with 37.7% contribution while contribution of PM_{2.5} and PM₁₀ reduced to nearly equal levels. PM₁₀ was the second highest contributor among the pollutants. The combined contribution of NO₂ and SO was 10% during both the 2015–2019 and 2020 period.

Summary and conclusion

The lockdown considerably reduced the level of O₃ precursor gases and PM and BC. The positivity is somewhat diluted by the simultaneous increase in O₃, a major pollutant. The variations are ascribed to the near total absence of anthropogenic activities only, specially the vehicular movement. However, industries like thermal power plants, oil and gas fields were active throughout the lockdown period. The impact of change in solar flux and meteorology during the 40-day period has not been considered, keeping in mind that there are less year to year variations in average meteorology over the region. Further, the contribution from distant and local sources to the pollutant load over a selected location can be quantitatively estimated provided there are *in situ* measurements at the source and receptor sites¹⁵. In that paper, the export efficiencies of NO_x, CO₂, CO, BC from identified major

source regions IGP and BoB have been estimated on the basis of available emission inventory but quantification was not attempted due to the reason cited above. In a recent work, using the WRF-STEM model¹⁶ it has been established that the North-Eastern Indian states contribute to the anthropogenic CO level by 59% in all seasons throughout the year (in 2013) followed by China, IGP, BoB and rest of Indian subcontinent. The local biomass burning in northeast India contributes to 90% of CO during pre-monsoon season. Thus, for this brief lockdown period the modelling exercise was not performed. The fact that forced reduction in anthropogenic activity can mitigate the negative effect of pollution on climate a great deal is to be taken in right perspective by policy planners and governments.

- Shi Xiaoqin and Brasseur, G. P., The response in air quality to the reduction of Chinese economic activities during the COVID-19 outbreak. *Geophys. Res. Lett.*, 2020; doi:10.1029/2020GL088070.
- Xu Kaijie, Kangping Cui, Li-Hao Young, Yen-Kung Hsieh, Ya-Fen Wang, Jiajia Zhang and Shun Rocky Wan, Impact of the COVID-19 event on air quality in Central China. *Aerosol Air Qual. Res.*, 2020, **20**, 915–929; doi:10.4209/aaqr.2020.04.0150.
- Bauwens, M. *et al.*, Impact of coronavirus outbreak on NO₂ pollution assessed using TROPOMI and OMI observations. *Geophys. Res. Lett.*, 2020; doi:10.1029/2020GL087978.
- Sharma, S., Zhang, M., Gao, J., Zhang, H. and Kota, S. H., Effect of restricted emissions during COVID-19 on air quality in India. *Sci. Total Environ.*, 2020, **728**, 138878.
- Mahato, S., Pal, S. and Ghosh, K. G., Effect of lockdown amid COVID-19 pandemic on air quality of the megacity Delhi, India. *Sci. Total Environ.*, 2020, **730**, 139086.
- Pathak, B., Bhuyan, P. K., Biswas, J. and Takemura, T., Long term climatology of particulate matter and associated microphysical and optical properties over Dibrugarh, North-East India and inter-comparison with SPRINTARS simulations. *Atmos. Environ.*, 2013, **69**, 334–344.
- Pathak, B. and Bhuyan, P. K., Absorbing and scattering properties of boundary layer aerosols over Dibrugarh, Northeast India. *Int. J. Remote Sensing*, 2014, **35**(14), 5527–5543.
- Bhuyan, P. K., Bharali, C., Pathak, B. and Kalita, G., The role of precursor gases and meteorology on temporal evolution of O₃ at a tropical location in North East India. *Environ. Sci. Poll. Res.*, 2014, 1–18; doi:10.1007/s11356-014-2587-3.
- Gogoi, M. M. *et al.*, Radiative effects of absorbing aerosols over Northeastern India: observations and model simulations. *J. Geophys. Res. Atmos.*, 2017, **122**, 1132–1157.
- Pathak, B., Borah, D., Khataniar, A., Bhuyan, P. K. and Buragohain, A. K., Characterization of bioaerosols in Northeast India in terms of culturable biological entities along with inhalable, thoracic and alveolar particles. *J. Earth Syst. Sci.*, 2020, **219**, 141; https://doi.org/10.1007/s12040-020-01406-z.
- Gogoi, M. M., Krishna Moorthy, K., Babu, S. S. and Bhuyan, B. K., Climatology of columnar aerosol properties and the influence of synoptic conditions: First-time results from the northeastern region of India. *J. Geophys. Res.: Atmospheres*, 2009, **114**(D8); https://doi.org/10.1029/2008JD010765.
- Gogoi, M. M., Pathak, B., Moorthy, K. K., Bhuyan, P. K., Babu, S. S., Bhuyan, K. and Kalita, G., Multi-year investigations of near surface and columnar aerosols over Dibrugarh, north-eastern location of India: Heterogeneity in source impacts. *Atmos. Environ.*, 2011, **45**(9), 1714–1724.
- Pathak, B., Bhuyan, P. K., Gogoi, M. M. and Bhuyan, K., Seasonal heterogeneity in aerosol types over Dibrugarh, North-Eastern India. *Atmos. Environ.*, 2012, **47**, 307–315; doi:10.1016/j.atmosenv.2011.10.061.
- Pathak, B. *et al.*, Aerosol characteristics in north-east India using ARFINET spectral optical depth measurements. *Atmos. Environ.*, 2016, **125**(B), 461–473.
- Binita, P., Chutia, L., Bharali, C. and Bhuyan, P. K., Continental export efficiencies and delineation of sources for trace gases and black carbon in North-East India: Seasonal variability. *Atmos. Environ.*, 2016; http://dx.doi.org/10.1016/j.atmosenv.2015.09.020.
- Saikia, A., Pathak, B., Singh, P., Bhuyan, P. K. and Adhikary, B., Multi-model evaluation of meteorological drivers, air pollutants and quantification of emission sources over the Upper Brahmaputra basin. *Atmosphere*, 2019, **10**(11), 703.
- Dahutia, P., Pathak, B. and Bhuyan, P. K., Aerosols characteristics, trends and their climatic implications over Northeast India and adjoining South Asia. *Int. J. Climatol.*, 2018, **38**, 1234–1256.
- Girach, I. A., Nair, P. R., Ojha, N. and Sahu, L. K., Tropospheric carbon monoxide over the northern Indian Ocean during winter: influence of inter-continental transport. *Climate Dyn.*, https://doi.org/10.1007/s00382-020-05269-4.
- Stortini, M., Arvani, B. and Deserti, M., Operational forecast and daily assessment of the air quality in Italy: a Copernicus-CAMS downstream service. *Atmosphere*, 2020, **11**, 447; doi:10.3390/atmos11050447.
- Pathak, B., Kalita, G., Bhuyan, K., Bhuyan, P. K. and Moorthy, K. K., Aerosol temporal characteristics and its impact on shortwave radiative forcing at a location in the northeast of India. *J. Geophys. Res.: Atmosphere*, 2010, **115**(D19).
- Gogoi, M. M. *et al.*, Air-borne *in-situ* measurements of aerosol size I distributions and BC across the IGP during SWAAMI. *Atmospheric Chemistry and Physics Discussion*, 2020; https://doi.org/10.5194/acp-2020-144.
- Sen, P. K., Estimates of the regression coefficient based on Kendall's tau. *J. Am. Statist. Assoc.*, 1968, **63**, 1379–1389.
- Lin, S., Trainer, M. and Liu, S. C., On the nonlinearity of the tropospheric ozone production. *J. Geophys. Res.*, 1988, **93**, 15879.
- Seinfeld, J. H. and Pandis, S. N., *Atmospheric Chemistry and Physics: From Air Pollution to Climate Change*, John Wiley and Sons, 2006.
- Crutzen, P. J., Lawrence, M. G. and Poschl, U., On the background photochemistry of tropospheric ozone. *Tellus*, 1999, **A51**, 123–146; doi:10.1034/j.1600-0870.1999.t01-1-00010.x.
- Logan, J. A., Prather, J. J., Wofsy, S. C. and McElroy, M. B., Tropospheric chemistry: A global perspective. *J. Geophys. Res.*, 1981, **86**, 7210–7254; doi:10.1029/JC086iC08p07210.
- Control of Urban Pollution Series: CUPS/82/2014-15.

ACKNOWLEDGEMENTS. We acknowledge the Indian Space Research Organisation for providing infrastructure facilities under its two major programmes ARFI and EOP (formerly ATCTM) operational under GBP. A.S. and P. Ajay thank ISRO for providing fellowship. This work was carried out within the broad terms of reference of the HICAB project supported by DST, India. The support provided by the UGC under SAP DRS II for procurement of the nano-SMPS is thankfully acknowledged.

doi: 10.18520/cs/v120/i2/322-331